

Photonic Bloch oscillations and Wannier-Stark ladders in exponentially chirped Bragg gratings

P. B. Wilkinson

School of Physics and Astronomy, University of Nottingham, Nottingham, NG7 2RD, United Kingdom

(Received 18 December 2001; published 20 May 2002)

The formation of photonic Bloch oscillations and Wannier-Stark ladders is demonstrated in an exponentially chirped one-dimensional Bragg grating. The photonic Bloch oscillations are investigated using Hamiltonian optics, and direct analogies are made with electron dynamics in periodic potentials. The results of transfer matrix calculations are presented, which show the existence of a photonic Wannier-Stark ladder that should be detectable in experiments.

DOI: 10.1103/PhysRevE.65.056616

PACS number(s): 42.15.-i, 42.70.Qs, 45.20.Jj, 42.25.-p

Traditionally, a Bloch oscillation is regarded as the semiclassical motion of a charged particle in a periodic potential subject to a uniform electric field. The field accelerates the particle through the energy band formed by the periodic potential. When the particle reaches the Brillouin zone boundary, it is Bragg reflected. It is then decelerated by the field until it comes to rest, completing one period of the oscillation. Although this phenomenon was predicted by Bloch in 1928 [1], it has only recently been observed directly in high-quality semiconductor superlattices [2,3]. The quantization of this semiclassical motion leads to equally spaced sequences of energy levels known as Wannier-Stark ladders [4], which have also been directly detected [5,6].

Recently, several optical systems have been proposed and studied which exhibit photonic Bloch oscillations and Wannier-Stark ladders. In these systems, the photonic lattice and its frequency bands change with position. This causes the Bloch wave vector of the light to change as it propagates through the photonic structure, mimicking the effects of external fields on a charged particle in a periodic potential. The first experimental observation of a photonic Wannier-Stark ladder used a linearly chirped Moiré grating written in the core of an optical fiber [7,8]. The grating had two slightly different periodicities, both of which were linearly chirped. The beating of the two periods formed a linearly ramped photonic band with a periodically modulated bandwidth. The linear ramp produced one of the turning points of the Bloch oscillation whilst the periodic modulation produced the second. Other studies have proposed using a linear variation of refractive index superimposed on an unchirped Bragg grating comprising high and low index layers [9–11]. Optical Bloch oscillations have been observed in experiments on two-dimensional waveguide arrays using this index profile [12,13]. Finally, unchirped Bragg gratings with a slowly varying lateral confinement have also been shown to produce photonic Bloch oscillations [14] and a Wannier-Stark ladder [15].

In this paper, a simple geometry is proposed which produces photonic Bloch oscillations and exhibits an equally spaced Wannier-Stark ladder. The system is a Bragg grating which is chirped *exponentially*, as opposed to the more common linearly chirped grating. Physical insight into the nature of the photonic Bloch oscillations is provided by a Hamiltonian optics analysis, which is directly analogous to the semiclassical description of electronic Bloch oscillations in a

periodic potential. The results of transfer matrix calculations are presented, which demonstrate the existence of the photonic Wannier-Stark ladder and suggest that a subset of the Wannier-Stark resonances could be probed by simple optical transmission experiments.

Figure 1 shows the unit cells, lattices, and local band structures of a simple semiconductor superlattice and the exponentially chirped Bragg grating considered in this paper. The semiconductor superlattice shown in Fig. 1(b) is formed from the unit cell shown by solid lines in Fig. 1(a). The overall width of the unit cell is l and the width of the potential barrier is d . The superlattice is subject to a uniform electric field $F \propto -dU/dx$ where $U(x)$ is the corresponding lin-

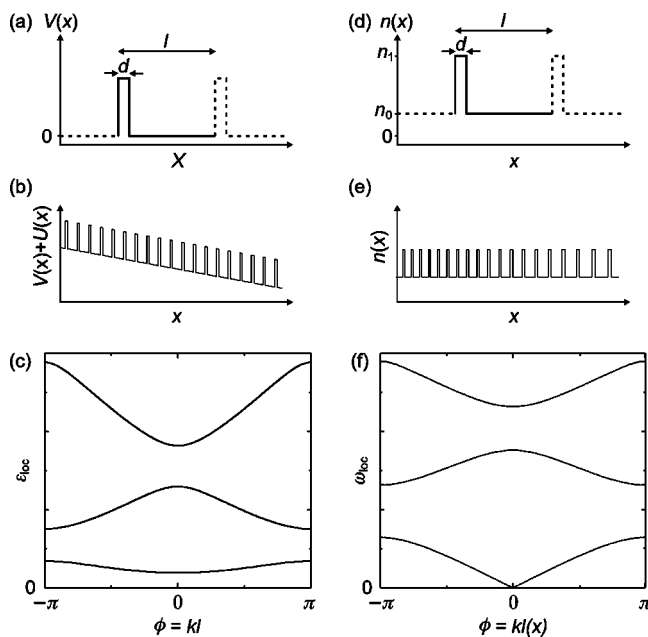


FIG. 1. (a) Potential energy profile $V(x)$ of the unit cell of a uniform semiconductor superlattice. (b) Potential energy profile of the semiconductor superlattice in the presence of a uniform electric field. (c) Reduced zone representation of the local energy band structure ϵ_{loc} of the superlattice in a uniform electric field. (d) Refractive index profile $n(x)$ of the unit cell of the uniform Bragg grating. (e) Refractive index profile of an exponentially chirped Bragg grating. (f) Reduced zone representation of the local frequency band structure ω_{loc} of the chirped grating. Any unspecified units and scales are arbitrary.

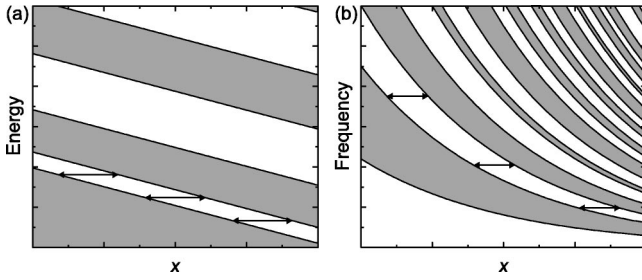


FIG. 2. (a) Energy bands (white) and band gaps (gray) of the superlattice shown in Fig. 1(b) as a function of position. (b) Frequency bands (white) and band gaps (gray) of the exponentially chirped Bragg grating shown in Fig. 1(e). In both cases the solid lines with arrowheads indicate the extent of Bloch oscillations at particular energies or frequencies. All units and scales are arbitrary.

ear potential energy. Providing that the potential energy drop across the unit cell is small, a local energy band structure ϵ_{loc} is formed for semiclassical motion in the lattice. This is shown in a reduced zone representation in Fig. 1(c) as a function of $\phi = kl$, where k is the Bloch wave number. At a given position x , $\epsilon_{\text{loc}}(\phi) = E(\phi) + U(x) - U(x_0)$, where $E(\phi)$ is the local band structure at $x = x_0$. As an electron moves through this superlattice, the local band structure is translated up and down in energy by the change in potential. The turning points of Bloch oscillations in the lattice are caused by Bragg reflection and they occur when the band edges coincide with the total energy of the electron, which is constant.

Figure 1(e) shows the refractive index profile of an exponentially chirped Bragg grating, in which each cell resembles the unit cell shown by solid lines in Fig. 1(d). Whilst l is now a function of x , the ratio d/l is kept constant. If $l(x)$ varies slowly, a local frequency band structure ω_{loc} forms as shown in Fig. 1(f). Since Maxwell's equations scale linearly with frequency, $\omega_{\text{loc}}(\phi) = \Omega(\phi)l_0/l(x)$, where $\Omega(\phi)$ and l_0 are the band structure and unit cell size, respectively, at $x = x_0$. As the light propagates through the grating, the photonic band structure is scaled (as opposed to translated) up and down in frequency by the changing cell size. The turning points of the Bloch oscillation occur when the band edges equal the frequency of the light, which is a constant of the motion like the total energy of the electron in the superlattice. In this paper, exponentially chirped gratings are considered with

$$l(x) = l_0 \exp[\eta(x - x_0)], \quad (1)$$

where η is a small constant that determines the chirp rate. It will be shown that this profile causes Bloch oscillations with constant amplitudes and periods, and consequently a Wannier-Stark ladder with constant frequency spacings.

The dependence of the electronic and photonic band structures on position in the two systems is shown schematically in Fig. 2. Figure 2(a) shows the energy band edges as a function of x in the semiconductor superlattice. The white and gray regions indicate the bands and band gaps, respectively, whilst the solid lines with arrowheads indicate the extent of Bloch oscillations at specific energies. Since the

bands are all inclined at the same gradient by the uniform electric field, the periods ($\tau_B = h/eFl$, where e is the electronic charge) and amplitudes ($L_B = \Delta/eF$, where Δ is the bandwidth) of all the Bloch oscillations in a particular band are independent of the energy of the electron.

Similarly, Fig. 2(b) shows the frequency band edges of the exponentially chirped Bragg grating. In this case, as will be shown below, it is the exponential scaling of the bands which ensures that the Bloch oscillations have constant periods and frequencies. Note that the lowest photonic band edge is fixed at $\omega_{\text{loc}} = 0$ because the bands are scaled, unlike the lowest electronic band edge, which is shifted up or down by the applied field. This means that there can be no photonic Bloch oscillations in the lowest band of the grating because the frequency of the lowest band edge can never coincide with the frequency of the light. However, photonic Bloch oscillations do occur in all the other bands.

The existence of electronic Bloch oscillations in a periodic potential can be demonstrated by a semiclassical argument relating the force on the electron to the rate of change of the Bloch wave vector [4]. For the exponentially chirped Bragg grating, an analogous result can be derived using Hamiltonian optics. In this formalism [16], the paths of geometrical rays in slowly varying photonic band materials are determined from Hamilton's equations

$$\frac{d\mathbf{x}}{d\sigma} = \frac{\partial \mathcal{H}}{\partial \mathbf{k}} \quad (2)$$

and

$$\frac{d\mathbf{k}}{d\sigma} = -\frac{\partial \mathcal{H}}{\partial \mathbf{x}}, \quad (3)$$

where $\mathbf{x} = \{x, y, z, -ct\}$, $\mathbf{k} = \{k_x, k_y, k_z, \omega/c\}$, \mathcal{H} is the Hamiltonian, and σ is some measure of distance along the ray path. In this paper, it is assumed that the Bragg gratings are infinite and unchanging along y and z . The resulting one-dimensional (1D) Hamiltonian is derived directly from the local dispersion relation. For a ray path corresponding to an electromagnetic wave with angular frequency ω , the Hamiltonian is

$$\mathcal{H}(x, k, \omega) = \omega_{\text{loc}}(\phi) - \omega = \Omega(\phi) \frac{l_0}{l(x)} - \omega, \quad (4)$$

where $\phi = kl(x)$, $k = k_x$ and the scaled dispersion relation $\Omega(\phi) = \omega_{\text{loc}}(\phi)l(x)/l_0$ is independent of x . For any given ray path, Hamilton's equations ensure that x and k vary according to the condition $\mathcal{H} = 0$, implying $\omega_{\text{loc}}(\phi) = \omega$ at all times. To calculate the amplitudes and periods of Bloch oscillations in an exponentially chirped lattice, Eqs. (2) and (3) must be integrated with respect to t . The initial step is to substitute Eq. (4) into Eq. (2), which shows that $d/dt = d/d\sigma$ in this case. It is worth noting at this point that the scaled wave number ϕ is also the phase within the Bloch oscillation cycle (this will be illustrated later in Fig. 3). The rate of change of the phase is

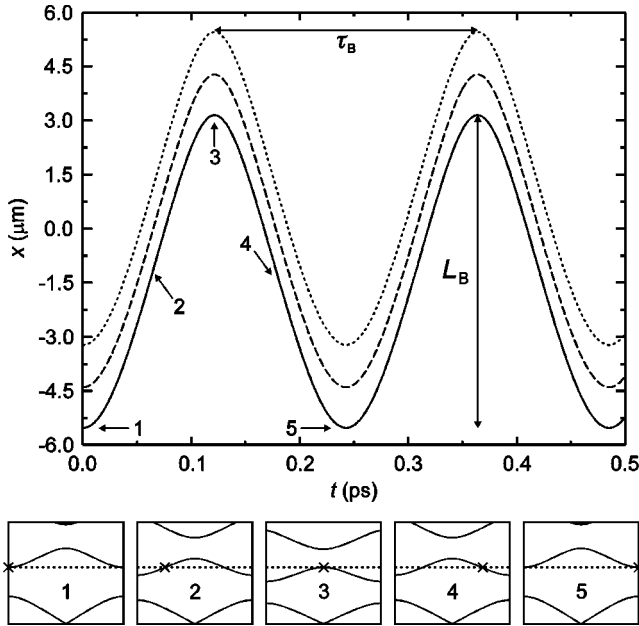


FIG. 3. Bloch oscillations in an exponentially chirped Bragg grating calculated for light rays with angular frequencies $\omega=2.7 \times 10^{15} \text{ rad s}^{-1}$ (solid), $\omega=2.6 \times 10^{15} \text{ rad s}^{-1}$ (dashed), and $\omega=2.5 \times 10^{15} \text{ rad s}^{-1}$ (dotted). The numbered plots below show the local dispersion relation $\omega_{\text{loc}}(\phi)$ at positions and times (x, t) indicated by the corresponding numbered arrows. In these plots, the dotted lines indicate the constant angular frequency of the light ω and the crosses show the phase of the Bloch oscillation ϕ at each coordinate (x, t) . The scales of the plots are the same as Fig. 1(f).

$$\frac{d\phi}{dt} = k \frac{dl}{dx} \frac{dx}{dt} + l(x) \frac{dk}{dt}. \quad (5)$$

Equations (2) and (3) give

$$\frac{dx}{dt} = \frac{l_0}{l(x)} \frac{\partial \Omega}{\partial k} = \frac{l_0}{l(x)} \frac{d\Omega}{d\phi} \frac{\partial \phi}{\partial k} = l_0 \frac{d\Omega}{d\phi}, \quad (6)$$

and

$$\begin{aligned} \frac{dk}{dt} &= - \left(\frac{l_0}{l(x)} \frac{\partial \Omega}{\partial x} + l_0 \Omega(\phi) \frac{d}{dx} \left[\frac{1}{l(x)} \right] \right) \\ &= - \left(\frac{l_0}{l(x)} \frac{d\Omega}{d\phi} \frac{\partial \phi}{\partial x} - \frac{l_0}{l^2(x)} \Omega(\phi) \frac{dl}{dx} \right) \\ &= \Omega(\phi) \frac{l_0}{l^2(x)} \frac{dl}{dx} - k \frac{dl}{dx} \frac{l_0}{l(x)} \frac{d\Omega}{d\phi}, \end{aligned} \quad (7)$$

respectively. Substituting Eqs. (6) and (7) into Eq. (5) gives

$$\frac{d\phi}{dt} = \Omega(\phi) \frac{l_0}{l} \frac{dl}{dx}. \quad (8)$$

The rate of change of phase determines the amplitudes L_B and periods τ_B of the photonic Bloch oscillations. If $d\phi/dt$ is a function of ϕ and constant terms *only*, then L_B and τ_B for Bloch oscillations in a given band are independent of x , and consequently independent of ω . This condition is satisfied

provided that $dl/dx \propto l$, which is clearly the case when $l(x)$ is given by Eq. (1). For this exponential chirp profile, the rate of change of phase reduces to

$$\frac{d\phi}{dt} = \eta l_0 \Omega(\phi). \quad (9)$$

The amplitude is found by integrating $dx/d\phi$ between the left- and right-hand limits of the Bloch oscillation ($\phi = -\pi$ and $\phi = 0$, respectively). This gives

$$\begin{aligned} L_B &= \int_{-\pi}^0 \frac{dx}{dt} \left(\frac{d\phi}{dt} \right)^{-1} d\phi \\ &= \frac{1}{\eta} \int_{-\pi}^0 \frac{1}{\Omega(\phi)} \frac{d\Omega}{d\phi} d\phi \\ &= \frac{1}{\eta} \ln \left(1 + \frac{\Delta_0}{\Omega_0} \right), \end{aligned} \quad (10)$$

where $\Omega_0 = \Omega(-\pi)$ is the lower edge of the band at $x = x_0$ and $\Delta_0 = \Omega(0) - \Omega_0$ is the corresponding bandwidth. Similarly, the period of the Bloch oscillation is found by integrating $dt/d\phi$ over one cycle ($\phi = 0 \rightarrow 2\pi$), giving

$$\tau_B = \int_0^{2\pi} \left(\frac{d\phi}{dt} \right)^{-1} d\phi = \frac{1}{\eta l_0} \int_0^{2\pi} \frac{1}{\Omega(\phi)} d\phi. \quad (11)$$

For any given band, Eqs. (10) and (11) demonstrate that L_B and τ_B are independent of ω . Although L_B is simply a function of the band edge frequencies at x_0 , τ_B depends on the form of $\Omega(\phi)$ throughout the band and must usually be calculated numerically. However, when the ratio n_1/n_0 is large, the dispersion relation can be approximated to $\Omega(\phi) \approx \Omega_0 + \Delta_0(1 + \cos \phi)/2$ [8]. In this approximation $\tau_B \approx 2\pi/\eta l_0 \Omega_0 (1 + \Delta_0/\Omega_0)^{1/2}$.

It is important to note that L_B and τ_B will be constant for *any* general $\Omega(\phi)$ that has nonzero upper and lower band edges and varies monotonically between them. Any 1D periodic structure that exhibits such a photonic band could have a slow exponential chirp applied to it. It would then support photonic Bloch oscillations with constant periods and amplitudes. The analogies between these Bloch oscillations and their electronic counterparts are very strong. They occur in 1D as a function of time, with amplitudes and periods that are independent of frequency within the same band. By contrast, in some previous studies, the Bloch oscillations can only occur in 2D. This is because one of the turning points is caused either by a total internal reflection [9–13], or by varying the width of the sample in the second direction [14,15]. Also, in one of the systems [11], the periods and amplitudes of the Bloch oscillations depend on frequency.

The chirped grating considered in this paper consists of the simple Krönig-Penney model unit cells shown in Fig. 1(d). Three Bloch oscillations in the same photonic band of this grating are shown in Fig. 3. They were generated by numerically integrating Eqs. (2) and (3) using a fourth-order Runge-Kutta method. Since l is assumed to vary slowly with x , the scaled dispersion relation $\Omega(\phi)$ in the chirped grating

is approximately the same as that of an unchirped grating with constant cell size l_0 . Using this approximation, $\Omega(\phi)$ was found by solving the transcendental equation

$$\begin{aligned} \cos(\phi) = & \cos\left(\frac{\Omega n_1}{c} d_0\right) \cos\left(\frac{\Omega n_0}{c} (l_0 - d_0)\right) \\ & - \frac{1+r^2}{2r} \sin\left(\frac{\Omega n_1}{c} d_0\right) \sin\left(\frac{\Omega n_0}{c} (l_0 - d_0)\right), \end{aligned} \quad (12)$$

where $r = n_1/n_0$ [17]. The parameters were $x_0 = 0$, $l_0 = 0.3 \mu\text{m}$, $d_0 = 0.1 \mu\text{m}$, $\eta = 3.333 \times 10^4 \text{ m}^{-1}$, $n_0 = 1.0$, and $n_1 = 3.5$. The low index layers are air, and the high index layers are GaAs. For the Bloch oscillations to occur, the local tolerance on the width of each layer would have to be an order of magnitude less than the difference in size between neighboring cells. Similar photonic lattices with features on these scales have been made in 1D by electron-beam lithography and etching of an epitaxially grown $\text{Al}_x\text{Ga}_{1-x}\text{As}$ wafer [18]. Photonic Bloch oscillations were investigated in the first excited band, for which $\Omega_0 = 2.248 \times 10^{15} \text{ rad s}^{-1}$ and $\Delta_0 = 0.755 \times 10^{15} \text{ rad s}^{-1}$. The angular frequency range used in Fig. 3 was $2.5 \times 10^{15} \text{ rad s}^{-1} \leq \omega \leq 2.7 \times 10^{15} \text{ rad s}^{-1}$. The numerically calculated periods and amplitudes of all three Bloch oscillations are $\tau_B = 0.2426 \text{ ps}$ and $L_B = 8.688 \mu\text{m}$, respectively. As predicted, they are independent of ω and agree exactly with the results of Eqs. (10) and (11).

The numbered plots at the base of Fig. 3 demonstrate that ϕ is the phase of the Bloch oscillation. They show the local dispersion relations $\omega_{\text{loc}}(\phi)$ at positions x and times t indicated by the corresponding numbered arrows. The dotted lines mark the optical frequency ω , which is a constant of the motion, and the crosses indicate ϕ . The ray path starts at $\phi = -\pi$ (plot 1) and moves in the positive x direction (plot 2) since the group velocity given by Eq. (6) is positive. At $\phi = 0$ (plot 3) the ray has moved far enough towards positive x that the upper edge of the band is equal to ω causing the ray to be Bragg reflected. The ray now has a negative group velocity, and it moves back towards negative x (plot 4) until it reaches $\phi = \pi$ (plot 5). At this point, it Bragg reflects from the lower edge of the band, completing the cycle.

The Hamiltonian approach gives good physical insight into the origin and nature of the photonic Bloch oscillations in this geometry, but it can only be validated by a comparison with the solution of Maxwell's equations. Since the Bragg gratings are assumed to be infinite in extent along y and z , electromagnetic waves moving in 1D along x obey a scalar wave equation

$$\nabla^2 \psi + \frac{\omega^2 n^2}{c^2} \psi = 0, \quad (13)$$

where ψ is either the electric or magnetic field vector perpendicular to the interfaces. To produce the exponential chirp specified by Eq. (1), the length of the j th cell, L_j , is determined by solving $\int_{x_j}^{x_{j+1}} \exp(-\eta(x-x_0)) dx = l_0$ for x_{j+1} , where x_j is the known left-hand edge of the cell, x_{j+1} is the

right-hand edge, and $L_j = x_{j+1} - x_j$. If the left-hand edge of cell 0 is at x_0 then it is straightforward to show that

$$x_j = x_0 - \frac{\ln(1-j\eta l_0)}{\eta} \quad (14)$$

and

$$L_j = -\frac{1}{\eta} \ln\left(1 - \frac{\eta l_0}{1-j\eta l_0}\right). \quad (15)$$

By applying the approximation

$$\ln(1-s) \approx \frac{\ln(1+s)}{\ln(1+s)-1}, \quad (16)$$

which is exact up to and including the third power of s , to Eq. (15) it is possible to derive the simple recursive relation

$$L_j \approx \frac{L_{j-1}}{1 - \eta L_{j-1}}. \quad (17)$$

Equation (17) is extremely accurate for the slowly chirped gratings that are considered in this paper. In a recent paper [15], a 1D photonic lattice was proposed that generated Bloch oscillations and a Wannier-Stark ladder using this same relation. Each cell of the lattice was formed from a high index well region with a Bragg mirror on each end. The fields in these cells were localized strongly in the well regions, and coupled only weakly to adjacent cells by the evanescent fields in the Bragg mirrors. This allowed the authors of [15] to derive a relation equivalent to Eq. (17) from a tight binding argument. But the Hamiltonian optics analysis presented here is more general. It predicts that *any* exponentially chirped lattice will exhibit photonic Bloch oscillations and Wannier-Stark ladders, including much simpler lattices than were used in [15].

To demonstrate the formation of a photonic Wannier-Stark ladder, Eq. (13) was solved for a 1D chirped Bragg grating with cell sizes related by Eq. (17) and parameters identical to those used for Fig. 3. The length of the grating was $17.9 \mu\text{m}$ and it was centered on $x = x_0$. The ends were assumed to be perfectly reflecting so that the confined eigenmodes of the grating could be calculated. A transfer matrix method was used to determine the angular frequencies of all the eigenmodes in the range $2.4 \times 10^{15} \text{ rad s}^{-1} \leq \omega \leq 2.8 \times 10^{15} \text{ rad s}^{-1}$. These are shown on the left-hand side of Fig. 4. At these frequencies, the electromagnetic fields are concentrated near the center of the grating and are very small near the ends. Therefore the eigenmodes can be identified with a Wannier-Stark ladder, even though this is strictly defined as the set of eigenmodes of an infinite lattice.

In semiconductor superlattices, the Wannier-Stark ladder originates from the quantization of the Bloch oscillations. The constant energy spacing of the states is related to the constant period of the Bloch oscillations by the Correspondence Principle, $\Delta E = h/\tau_B = eFl$. Similarly, in the chirped Bragg grating, the eigenmodes that have negligibly small amplitudes at the ends of the grating form a photonic Wannier-Stark ladder with a constant angular frequency

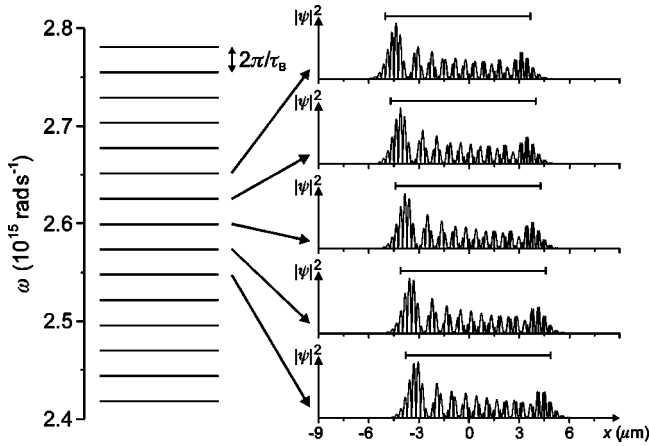


FIG. 4. Angular frequencies (left) of eigenmodes of an exponentially chirped Bragg grating with reflective ends. The eigenmodes are separated by $\Delta\omega = 2\pi/\tau_B$. The intensities of the fields in five of the modes are shown plotted (in arbitrary units) as a function of position x on the right. The solid bars above the intensity plots indicate the position and extent of the Bloch oscillations predicted by Hamiltonian optics.

spacing of $\Delta\omega = 2\pi/\tau_B$. In Fig. 4, $\Delta\omega = 2.590 \times 10^{13} \text{ rad s}^{-1}$ which agrees exactly with $2\pi/\tau_B = 2.590 \times 10^{13} \text{ rad s}^{-1}$ ($\tau_B = 0.2426 \text{ ps}$). On the right of Fig. 4 the field intensity profiles of five of the modes are shown as a function of position. The solid bar above each plot shows the position and extent ($L_B = 8.688 \mu\text{m}$) of the corresponding Bloch oscillation obtained from Hamiltonian optics. The agreement between the positions of the modes and the Bloch oscillations is extremely good, and it demonstrates the validity of the Hamiltonian optics analysis of this system. The modes are slightly longer than the Bloch oscillations as they have an evanescent tail at each end, which penetrates into the region within the band gap, which is forbidden to the geometrical ray path.

The evanescent sections of the eigenmodes should permit the experimental observation of the Wannier-Stark ladder over a small frequency range [19]. Figure 5 shows the transmission coefficient T of a chirped Bragg grating, centered on x_0 , which is identical to that used in Fig. 4 except that it does not have reflective ends and it has been shortened to $11.6 \mu\text{m}$. This length is slightly larger than L_B and was chosen such that the evanescent tails of the Wannier-Stark ladder modes localized near the center of the grating would just reach the ends. Transmission through this grating is possible

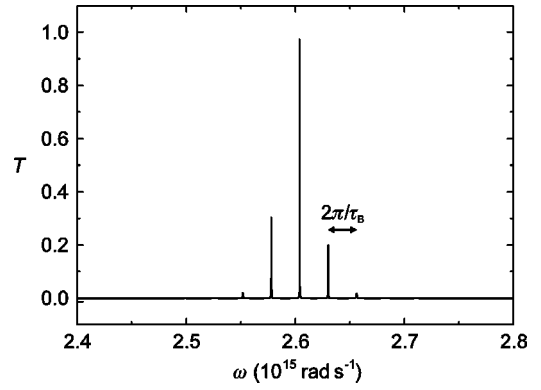


FIG. 5. Transmission coefficient $T(\omega)$ showing transmission peaks separated by $\Delta\omega \approx 2\pi/\tau_B$.

because the tails couple light from incident and transmitted plane waves at either end into and out of the Wannier-Stark ladder modes. The transfer matrix method was used to calculate $T(\omega)$ for the light incident on one of the ends. Five clear peaks are visible in Fig. 5, with a near-constant separation of $\Delta\omega \approx 2.61 \times 10^{13} \text{ rad s}^{-1}$. These peaks can be identified with resonant transmission through the modes of the Wannier-Stark ladder. The modes are only slightly perturbed by the finite length of the grating, which explains the small deviation of $\Delta\omega$ from the predicted value of $2\pi/\tau_B = 2.590 \times 10^{13} \text{ rad s}^{-1}$.

In conclusion, a simple geometry for producing photonic Bloch oscillations and Wannier-Stark ladders has been proposed: a slow exponential scaling of unit cell size with position in a *general* 1D photonic lattice. Simple expressions for the periods and amplitudes of the Bloch oscillations were derived using a Hamiltonian optics analysis. These photonic Bloch oscillations are directly analogous to their electronic counterparts since, within the same band, they all have the same period and amplitude independent of the frequency of the light. A photonic Wannier-Stark ladder with constant frequency spacings was also shown to exist in this system. The spatial extent and frequency spacing of the modes of the Wannier-Stark ladder agreed very closely with those predicted by quantizing the corresponding Bloch oscillations. With an appropriately designed grating, the Wannier-Stark modes should be experimentally detectable in transmission measurements over a narrow range of frequencies.

I would like to thank Dr. T. M. Fromhold for useful discussions. This work was funded by EPSRC U.K.

-
- [1] F. Bloch, *Z. Phys.* **52**, 555 (1928).
 - [2] J. Feldmann *et al.*, *Phys. Rev. B* **46**, R7252 (1992).
 - [3] C. Waschke *et al.*, *Phys. Rev. Lett.* **70**, 3319 (1993).
 - [4] G. H. Wannier, *Elements of Solid State Theory* (Cambridge University Press, London, 1959).
 - [5] E. E. Mendez, F. Agulló-Rueda, and J. M. Hong, *Phys. Rev. Lett.* **60**, 2426 (1988).
 - [6] M. M. Dignam and J. E. Sipe, *Phys. Rev. Lett.* **64**, 1797 (1990).
 - [7] C. Martijn de Sterke *et al.*, *Phys. Rev. E* **57**, 2365 (1998).
 - [8] I. Talanina and C. Martijn de Sterke, *Phys. Rev. A* **63**, 053802 (2001).
 - [9] G. Monsivais, M. del Castillo-Mussot, and F. Claro, *Phys. Rev. Lett.* **64**, 1433 (1990).
 - [10] U. Peschel, T. Pertsch, and F. Lederer, *Opt. Lett.* **23**, 1701 (1998).
 - [11] G. Lenz, I. Talanina, and C. Martijn de Sterke, *Phys. Rev. Lett.* **83**, 963 (1999).

- [12] T. Pertsch *et al.*, Phys. Rev. Lett. **83**, 4752 (1999).
- [13] R. Morandotti *et al.*, Phys. Rev. Lett. **83**, 4756 (1999).
- [14] A. Kavokin *et al.*, Phys. Rev. B **61**, 4413 (2000).
- [15] G. Malpuech *et al.*, Phys. Rev. B **63**, 035108 (2001).
- [16] P. St. J. Russell and T. A. Birks, J. Lightwave Technol. **17**, 1982 (1999).
- [17] T. J. Shepherd, P. J. Roberts, and R. Loudon, Phys. Rev. E **55**, 6024 (1997).
- [18] T. F. Krauss *et al.*, IEEE Photonics Technol. Lett. **9**, 176 (1997).
- [19] Whilst experimental observation of the photonic Bloch oscillations in a 1D system would be extremely difficult, it should be possible to observe them using an appropriately chirped 2D waveguide array as in [12,13].